Application of DBR Mode-Locked Lasers in Millimeter-Wave Fiber-Radio System

Tetsuichiro Ohno, *Member, IEEE*, Kenji Sato, *Member, IEEE*, Seiji Fukushima, *Member, OSA*, Yoshiyuki Doi, and Yutaka Matsuoka, *Member, IEEE*

***Abstract*—An actively mode-locked laser (MLLD) integrated with a distributed Bragg reflector (DBR) was used as a light source for optical subcarrier transmission. The millimeter (mm)-wave power penalty due to fiber dispersion is suppressed within 4 dB by operating this laser in a symmetric four-mode configuration. The experimental results agree well with the calculation of dispersion-induced penalty for a four-component-lightwave source. Optical subcarrier transmission free from dispersion-induced penalty within experimental error is achieved by further suppression of the end-modes of the DBR-MLLD using a fiber Bragg grating (FBG).**

***Index Terms*—Fiber Bragg gratings (FBG's), millimeter (mm)-wave generation, mode-locked lasers, optical fiber dispersion.**

I. Introduction

RECENTLY, millimeter radio waves have attracted much interest for wireless access systems, such as cellular networks or high-speed wireless local area networks. Higher frequency operation is desirable for broad-band wireless services. However, when millimeter (mm) waves are used, much attention should be paid to their generation and distribution. Fiber-radio systems [1], [2] exploit the ultralow loss and large bandwidth of optical fibers to distribute mm-waves. In these systems, light sources must convert mm-waves into the optical subcarrier efficiently. Semiconductor mode-locked lasers (MLLD) are promising for these sources because a large optical modulation index can be achieved for a relatively low input level. However, when a Fabry–Perot MLLD is used as a light source for optical subcarrier transmission, the transmitted power of mm-waves varies periodically with transmission distance due to second-order dispersion. A similar effect is also observed when an intensity modulator is used as an optical subcarrier source [3], and it imposes a strict limitation on the carrier frequency and the fiber length in fiber-radio systems. Optical single sideband modulation [4] or double-sideband modulation with suppressed carrier [5] can suppress the dispersion effects. However, these methods require a relatively high RF input level to obtain a large optical modulation index.

In this paper, we propose the use of an actively mode-locked laser integrated with a distributed Bragg reflector (DBR) [6] for the optical source in fiber-radio systems. By operating this MLLD under adequate conditions, the number of longitudinal modes can be reduced to only four, with both end-modes suppressed. From such a spectrum, it is expected that the dispersion effects can be reduced without lowering the optical modulation index. This paper is organized as follows. First, we present a theory of dispersion effects for a four-component-lightwave source. Next, the dispersion-induced penalty is shown to be less than 4 dB for the DBR-MLLD operating in only four modes. Finally, further suppression of end-modes of the DBR-MLLD using fiber Bragg grating (FBG) is shown to result in optical subcarrier transmission with negligible dispersion-induced penalty.

Manuscript received June 15, 1999; revised September 6, 1999.

T. Ohno, S. Fukushima, Y. Doi, and Y. Matsuoka are with NTT Photonics Laboratories, Kanagawa 243-0198, Japan (e-mail: tetuohno@aecl.ntt.co.jp).

K. Sato is with NTT Network Innovation Laboratories, Kanagawa 239-0847, Japan.

Publisher Item Identifier S 0733-8724(00)01465-1.

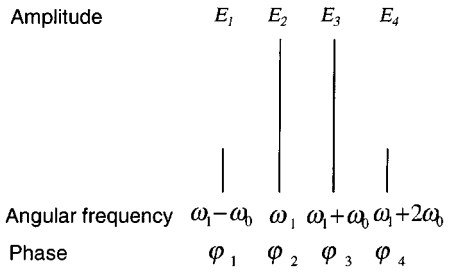

Fig. 1. Spectral model of the lightwave with four symmetrically configured components for the calculation.

II. Theory of Dispersion Effects for a Four-Component-Lightwave Source

Theories of dispersion effects for the conventional intensity modulator, which generates electric field of the lightwave with the carrier and double-sideband, have been reported in detail [3], [7]. In this section, we introduce a theory of dispersion effects for a lightwave with four components of different angular frequencies arranged in the same interval ω_0 corresponding to the desired millimeter (mm)-wave frequency. It is assumed that the optical spectrum of the lightwave is symmetric to a center frequency and both end-components are smaller than the center two components, as shown in Fig. 1. When the angular frequency of the second lower frequency component is defined as ω_1, total electric field $\mathbf{E}$ is written by

$$\mathbf{E} = E_1 e^{i\{(\omega_1-\omega_0)t+\varphi_1\}} + E_2 e^{i\{\omega_1 t+\varphi_2\}} + E_3 e^{i\{(\omega_1+\omega_0)t+\varphi_3\}} + E_4 e^{i\{(\omega_1+2\omega_0)t+\varphi_4\}} \quad (1)$$

where E_n and φ_n are the amplitude and phase of the nth component ($n = 1$–4, in frequency order) and t is time. Photocurrent

I generated by direct detection of the lightwave is proportional to $\mathbf{E}\cdot\mathbf{E}^*$ and is given by

$$\begin{aligned} I \propto (\mathbf{E}\cdot\mathbf{E}^*) = {} & E_1^2 + E_2^2 + E_3^2 + E_4^2 \\ & + 2E_1E_4\cos(3\omega_0 t + \varphi_4 - \varphi_1) \\ & + 2E_1E_3\cos(2\omega_0 t + \varphi_3 - \varphi_1) \\ & + 2E_2E_4\cos(2\omega_0 t + \varphi_4 - \varphi_2) \\ & + 2E_1E_2\cos(\omega_0 t + \varphi_2 - \varphi_1) \\ & + 2E_2E_3\cos(\omega_0 t + \varphi_3 - \varphi_2) \\ & + 2E_3E_4\cos(\omega_0 t + \varphi_4 - \varphi_3). \end{aligned} \tag{2}$$

Because we are interested in a mm-wave output with an angular frequency of ω_0, it is sufficient to take into account the sum of the three terms, which is written as b such that

$$\begin{aligned} b = {} & 2E_1E_2\cos(\omega_0 t + \varphi_2 - \varphi_1) + 2E_2E_3\cos(\omega_0 t + \varphi_3 - \varphi_2) \\ & + 2E_3E_4\cos(\omega_0 t + \varphi_4 - \varphi_3). \end{aligned} \tag{3}$$

In the optical fiber, each component of (1) propagates with different velocity due to fiber dispersion. The propagation constant β is expanded in a Taylor series up to the second order around the carrier frequency, and is given by

$$\beta \cong \beta_0 + \frac{2\pi\Delta f}{v_g} - \frac{\pi\lambda^2 D(\Delta f)^2}{c} \tag{4}$$

where

- β_0 propagation constant at the carrier frequency;
- Δf discrepancy from the carrier frequency;
- λ wavelength;
- v_g group velocity;
- D dispersion parameter [8].

When we take into account the linear chirp of the light source, we can write the phase of each component before propagation as $\varphi_1 = \chi((3/2)\omega_0)^2$, $\varphi_2 = \chi((1/2)\omega_0)^2$, $\varphi_3 = \chi((1/2)\omega_0)^2$, and $\varphi_4 = \chi((3/2)\omega_0)^2$. Here, χ is a temporal coefficient used to describe linear chirp. With propagation in a dispersive optical fiber, the phase of each component is changed to

$$\varphi_1 = \left(-\beta_0 + \frac{2\pi f_{\rm rf}}{v_g} + \frac{\pi\lambda^2 D f_{\rm rf}^2}{c}\right)L + \chi\left(\frac{3}{2}\omega_0\right)^2 \tag{5}$$

$$\varphi_2 = -\beta_0 L + \chi\left(\tfrac{1}{2}\omega_0\right)^2 \tag{6}$$

$$\varphi_3 = \left(-\beta_0 - \frac{2\pi f_{\rm rf}}{v_g} + \frac{\pi\lambda^2 D f_{\rm rf}^2}{c}\right)L + \chi\left(\frac{1}{2}\omega_0\right)^2 \tag{7}$$

$$\varphi_4 = \left(-\beta_0 - \frac{4\pi f_{\rm rf}}{v_g} + \frac{4\pi\lambda^2 D f_{\rm rf}^2}{c}\right)L + \chi\left(\frac{3}{2}\omega_0\right)^2 \tag{8}$$

where L is the fiber length and $f_{\rm rf} = \omega_0/2\pi$. Here, we take ω_1 as the carrier frequency in (4). Substituting (5)–(8) into (3), with amplitude defined as $E_1^2 = E_4^2 = rE_2^2 = rE_3^2$ using suppression ratio r, we obtain

$$\begin{aligned} b = {} & 2\sqrt{r}E_2^2[\cos(\omega_0 t + \varphi_2 - \varphi_1) + \cos(\omega_0 t + \varphi_4 - \varphi_3)] \\ & + 2E_2^2\cos(\omega_0 t + \varphi_3 - \varphi_2) \\ = {} & 2\sqrt{r}E_2^2 \times 2\cos\left(\omega_0 t - \frac{2\pi f_{\rm rf}L}{v_g} + \frac{\pi\lambda^2 D f_{\rm rf}^2 L}{c}\right) \\ & \times \cos\left(\frac{2\pi\lambda^2 D f_{\rm rf}^2 L}{c} + 2\chi\omega_0^2\right) \\ & + 2E_2^2\cos\left(\omega_0 t - \frac{2\pi f_{\rm rf}L}{v_g} + \frac{\pi\lambda^2 D f_{\rm rf}^2 L}{c}\right) \\ = {} & E_2^2\left[2 + 4\sqrt{r}\cos\left(\frac{2\pi\lambda^2 D f_{\rm rf}^2 L}{c} + 2\chi\omega_0^2\right)\right] \\ & \times \cos\left(\omega_0 t - \frac{2\pi f_{\rm rf}L}{v_g} + \frac{\pi\lambda^2 D f_{\rm rf}^2 L}{c}\right) \\ = {} & A(L)\cos\left(\omega_0 t - \frac{2\pi f_{\rm rf}L}{v_g} + \frac{\pi\lambda^2 D f_{\rm rf}^2 L}{c}\right). \end{aligned} \tag{9}$$

This equation shows that the amplitude of the photocurrent component with angular frequency ω_0 varies with fiber length as

$$A(L) = E_2^2\left[2 + 4\sqrt{r}\cos\left(\frac{2\pi\lambda^2 D f_{\rm rf}^2 L}{c} + 2\chi\omega_0^2\right)\right]. \tag{10}$$

As a result, the power of the RF signal with angular frequency ω_0 also varies as

$$P_{\rm rf}(L) \propto \tfrac{1}{2}RA(L)^2 \tag{11}$$

where R is load resistance. Dispersion-induced penalty in dB can be expressed as

$$\begin{aligned} \text{penalty} &= -10\log[P_{\rm rf}(L)/P_{\rm rf}(0)] \\ &= -10\log\left\{\frac{A(L)}{E_2^2[2 + 4\sqrt{r}\cos(2\chi\omega_0^2)]}\right\}^2 \end{aligned} \tag{12}$$

where $P_{\rm rf}(0)$ is the detected RF power before fiber transmission.

We could not introduce an equation for the dispersion-induced penalty when each end-component has different amplitude. However, in the case of a small difference, we confirm from numerical calculations that the penalty is almost the same as the penalty for the symmetric case in which both end-components have an averaged amplitude.

III. Experimental Setup

At first, we explain the DBR-MLLD [6] used as an optical transmitter in this experiment. Fig. 2 shows a schematic illustration of the DBR-MLLD. An electroabsorption (EA) modulator and a DBR are monolithically integrated in this laser. A constant bias current is injected into the gain section of the MLLD. The total cavity length of the MLLD is designed so that the resonant frequency becomes about 40 GHz. An optical subcarrier is generated by supplying a 40-GHz mm-waves to the EA modulator section together with a dc bias. The DBR is used as a front mirror. Without RF input for mode-locking, this laser operates in single mode at 1.551 μm where the reflectivity of the DBR has its maximum. When RF input is applied to the EA modulator section, the bandwidth of the optical spectrum increases with increasing RF input power. Therefore, by making the RF input power small enough, this laser can be operated with almost

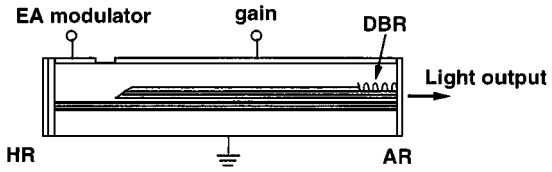

Fig. 2. Schematic illustration of the cross section of the DBR-MLLD used in this experiment.

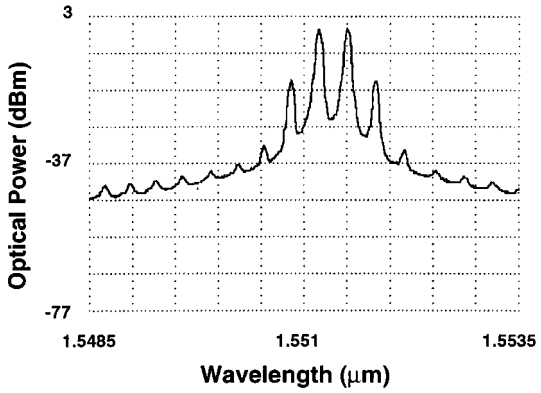

Fig. 3. Optical spectrum of the DBR-MLLD operating in the symmetric four-mode configuration.

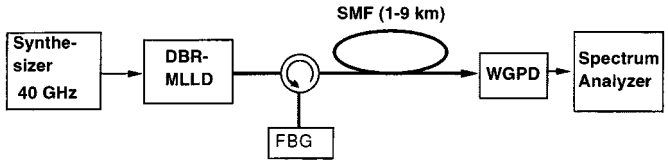

Fig. 4. Experimental setup for the measurements of dispersion-induced penalty for a fiber-optic link.

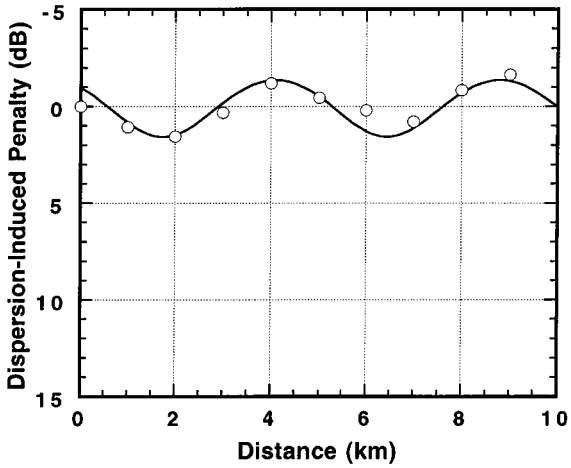

Fig. 5. Dispersion-induced penalty in the fiber-optic link using the DBR-MLLD as an optical subcarrier source. The DBR-MLLD was operated in the symmetric four-mode configuration (Fig. 3). The solid curve shows the value calculated from (12).

only four modes. Furthermore, the intensities of the two dominant modes can be equalized by adjusting the injection current, which would lead to a change in the refractive index of the gain section. By adjusting the operation conditions in such way, this laser can be operated with a spectrum that consists of two dominant modes and the other weak satellite modes. In this experiment, injection current into the gain section was 110 mA. The EA modulator section was driven with a 10 dBm RF signal superimposed on a reverse bias voltage of 1.0 V. The optical spectrum of the light output is shown in Fig. 3. Because the intensity of satellite modes is smaller than that of the dominant modes by 30 dB except for the strongest and the second strongest ones, this spectrum can be regarded as two dominant modes plus two end-modes as treated in the previous section. The optical spectrum is almost symmetric and both end-modes are much smaller than the center two modes. The center wavelength of the spectrum is about 1.5513 μm. From the spectrum, suppression of the dispersion effect can be expected. When this laser is operated under these conditions, the phase noise of the generated mm-wave carrier is −117 dBc/Hz at 1 MHz offset (−109 dBc/Hz at 100 KHz offset), which is dominated by the phase noise of the drive oscillator. The optical modulation index of the laser output, defined as the amplitude of the mm-wave component (40 GHz, in this paper) over averaged optical power, is 80%.

The dispersion-induced penalty of mm-waves was measured for the fiber optic link shown in Fig. 4. The optical subcarrier is generated by the DBR-MLLD described above. In some experiments, the output of the DBR-MLLD was further filtered in the spectral domain with a FBG. The optical signal was transmitted through a standard single-mode fiber with various lengths (1–9 km) and then detected by a waveguide p-i-n photodiode (WGPD) with 50-GHz bandwidth. The typical value of the dispersion parameter of the optical fibers used in our experiment was 16.70 ps/km/nm at 1.5513 μm. The output RF power of the WGPD was measured by an RF spectrum analyzer under a 50-Ω load condition. The dispersion-induced penalty was obtained by subtracting dc loss from the total RF power degradation caused by fiber transmission. The dc optical loss converted to photodiode output power loss was smaller than 4 dB throughout this experiment.

IV. Results and Discussion

The mm-wave power penalty due to fiber dispersion was measured for the fiber optic link with the DBR-MLLD operating in the symmetric four-mode configuration (Fig. 3). Fig. 5 shows the relationship between the transmission distance and the dispersion-induced penalty. The dispersion-induced penalty varies sinusoidally with a cycle of about 5 km. The variation of the mm-wave power is within 4 dB, which is much smaller than that appearing when the standard intensity modulator is used as an optical subcarrier source [3]. The solid curve in Fig. 5 shows the dispersion-induced penalty calculated using (12). In this calculation, $r = 0.01$ is used for the suppression ratio to fit the amplitude of the penalty. This value is a little smaller than that obtained from the optical spectrum ($r = 0.03$–0.04). To obtain the best fit with the experimental results, $\chi\omega_0^2$ is set at 0.13π and an offset of $+0.95$ dB is added to the vertical coordinate. Although the reason for this small offset is not clear, the variation of the calculated penalty well coincides with the measured ones. From the above result, it is confirmed that the sinusoidal variation of the penalty originates from the existence of the end-modes. By calculating the maximum penalty using

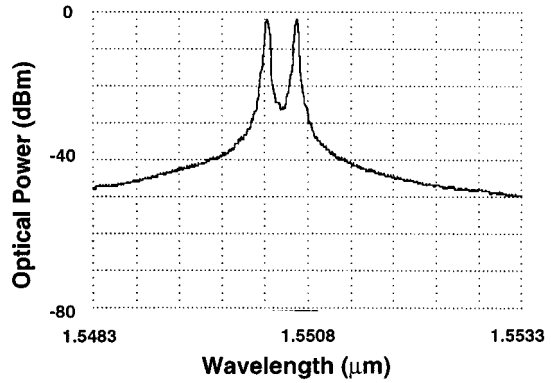

Fig. 6. Optical spectrum of the filtered light output of the DBR-MLLD using the FBG.

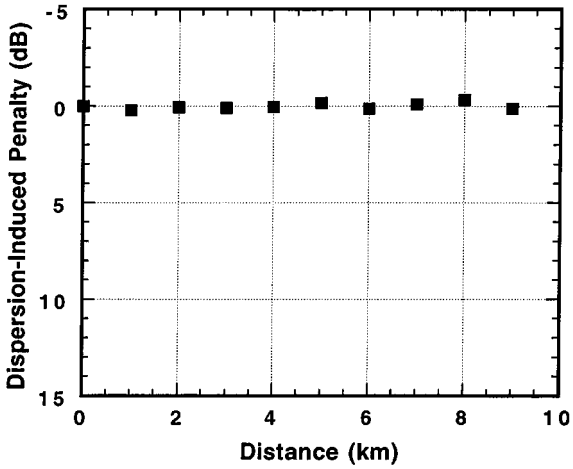

Fig. 7. Dispersion-induced penalty in the fiber-optic link using the DBR-MLLD together with the FBG.

(12), it is found that the suppression ratio should be larger than 30 dB to reduce the penalty within 1 dB.

Next, further reduction of the dispersion-induced penalty was attempted by using a FBG to suppress the end-modes of the DBR-MLLD. The reflectivity of the FBG is higher than 90% in the 40-GHz-wide spectral range centering at 1.5505 μm and lower than 1% at ±60 GHz from the center. Fig. 6 shows an optical spectrum of the output of the DBR-MLLD filtered by the FBG. In this experiment, the center wavelength of the light output from the DBR-MLLD was adjusted to agree with that of FBG reflectivity by changing ambient temperature. The spectrum consists of only two longitudinal modes with 40-GHz separation. The optical modulation index of the light from the FBG is about 70%. The value of the optical modulation index is lowered only 10% by the use of the FBG. The dispersion-induced penalty was measured for the DBR-MLLD used in combination with the FBG. Fig. 7 shows the dependence of the dispersion-induced penalty on transmission distance. Suppressing the end-modes of the DBR-MLLD and using only two center-modes reduces dispersion-induced penalty to ± 0.5 dB, which is within the range of the measurement error in this experiment.

In the above experiment, the FBG was just used as a spectral filter. Because the DBR integrated in the MLLD cavity also acts as a spectral filter, it is likely that the DBR-MLLD will be able to operate in only two modes by designing it appropriately. The FWHM bandwidth of the optical spectrum for the MLLD was about 0.7 nm when it was mode-locked with a strong enough RF signal (+20 dBm). This value is far smaller than the bandwidth of the DBR reflectivity (about 3 nm). Therefore, it is thought that the bandwidth of the optical spectrum is restricted by some factor other than the DBR spectrum. We consider that the dispersion of the DBR has to do with selectivity of the two dominant modes. Details of this mechanism will be reported elsewhere. If the DBR-MLLD could solely generate a light output with only two modes, and be free from dispersion-induced penalty, a very compact and cost-effective optical subcarrier source could be achieved. Therefore, the realization of two-mode DBR-MLLD would be very advantageous for practical use.

To show the applicability of the DBR-MLLD to fiber-radio systems, we also tried data transmission in the fiber optic link using this laser. Several methods are available to modulate output of the DBR-MLLD by digital signals; optical amplitude modulation by an external modulator, amplitude modulation of the injection current into the gain section of this laser [9], phase-shift-keying using optical delay switching [10], mode-locking with phase-modulated mm-waves, etc. Although it is very important to investigate the merits and demerits of these modulation methods, it is not the subject of this paper. So we used mode-locking with binary-phase-shift-keyed (BPSK) signal as an example to show the applicability of this laser to fiber-radio systems. Since the DBR-MLLD has a wide locking range [6], a BPSK formatted optical subcarrier can be directly generated as an output by mode-locking it with BPSK data. In the present work, the carrier frequency of the BPSK signal was 39.6 GHz and the data rate was 500 Mb/s. The BPSK signal was processed electrically and applied to the EA modulator section of the DBR-MLLD together with a reverse bias of 1.0 V. The power of the input BPSK signal was 14 dBm. The current injected into the gain section was 120 mA. The light output was converted into a mm-wave signal by the WGPD and then fed into the demodulator. A 2-m-long standard optical fiber was used to connect the laser and the WGPD. Digital output from the demodulator was amplified and fed into an error detector. Even in this case, the laser can be operated with an optical spectrum with two dominant modes and two other weak modes similar to those in Fig. 3. We also confirmed that the dispersion-induced penalty can be kept at a low level when the BPSK formatted optical signal is transmitted through a standard fiber shorter than 10 km. Fig. 8 shows an eye pattern of demodulated pseudorandom bit stream data. The received optical power was −7.4 dBm. The eye openings are wide and very well defined. From bit-error-rate (BER) measurements, BER was confirmed to be smaller than 10^{-11}.

Finally, we compare our present method with previously reported methods applied for the reduction of dispersion-induced penalty. First, we mention the dual-mode laser proposed by Wake *et al.* [11] The dual-mode laser is a kind of distributed feedback laser in which oscillation occurs simultaneously on both sides of the stop band. In this laser, because a set of sidebands is generated by subharmonic injection locking on both of the original optical modes, some pairs of components can produce beats with the same frequency as the beat frequency

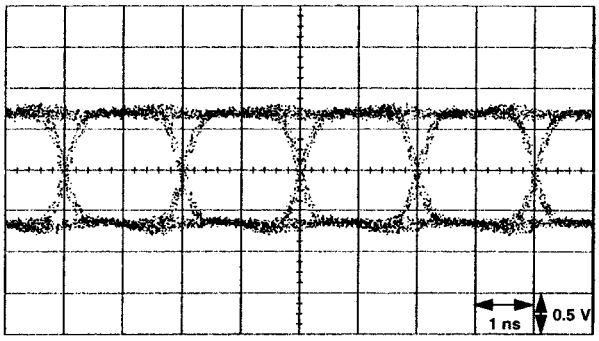

Fig. 8. Eye patterns of demodulated PRBS data.

of the original dual mode. When the output of this laser is transmitted through optical fiber, chromatic dispersion causes a phase-shift between these beats and, as a result, a power penalty of 5–20 dB is induced. If injection locking of this laser at the fundamental frequency is possible, the dispersion induced penalty will be suppressed. In optical double sideband modulation with a suppressed carrier [5], the original optical carrier is suppressed by biasing a standard Mach–Zehnder modulator at $V\pi$. However, in this method, very-high-power mm-waves with an amplitude comparable to $V\pi$ are required for modulator input to reduce the conversion loss of optical power due to the modulation. Another method is optical single-sideband modulation using combined balanced modulators [4]. This method also requires high-power mm-waves in order to achieve a large optical modulation index. In addition, because mm-waves with different phases are supplied to two balanced modulators, the amplitude and phase of the mm-waves have to be adjusted precisely. On the other hand, the present method requires only one mm-wave input with relatively low power of 10 dBm. The optical modulation index is as high as 80% under this condition.

V. Conclusion

Millimeter-wave power penalty due to fiber dispersion is reduced to within 4 dB by using a DBR-MLLD operating in symmetric four-mode configuration as an optical subcarrier source. Good agreement between the theoretical prediction for the four-component-lightwave source and the experimental results was confirmed. Optical subcarrier transmission free from dispersion-induced penalty within experimental error is achieved by using a FBG for further suppression of the end-modes of the DBR-MLLD.

Acknowledgment

The authors would like to thank S. Mitachi for his encouragement.

References

[1] H. Ogawa, "Microwave and millimeter-wave fiber optic technologies for subcarrier transmission systems," *IEICE Trans. Commun.*, vol. E76-B, pp. 1078–1090, 1993.
[2] W. E. Stephan and T. R. Joseph, "System characteristics of direct modulated and externally modulated RF fiber-optic links," *J. Lightwave Technol.*, vol. LT-5, pp. 380–387, 1987.
[3] F. Devaux, Y. Sorel, and J. F. Kerdiles, "Simple measurement of fiber dispersion and chirp parameter of intensity modulated light emitter," *J. Lightwave Technol.*, vol. 11, pp. 1937–1940, 1993.
[4] M. Izutsu, S. Shikama, and T. Sueta, "Integrated optical SSB modulator/frequency shifter," *IEEE J. Quantum Electron.*, vol. QE-17, pp. 2225–2227, 1981.
[5] H. Schmuck, R. Heidemann, and R. Hofstetter, "Distribution of 60 GHz signals to more than 1000 base stations," *Electron. Lett.*, vol. 30, pp. 59–60, 1994.
[6] K. Sato, A. Hirano, M. Asobe, and H. Ishii, "Chirp-compensated 40 GHz semiconductor modelocked lasers integrated with chirped gratings," *Electron. Lett.*, vol. 34, pp. 1944–1946, 1998.
[7] U. Gliese, S. Nørskov, and T. N. Nielsen, "Chromatic dispersion in fiber-optic microwave and millimeter-wave links," *IEEE Trans. Microwave Theory Tech.*, vol. 44, pp. 1716–1724, 1996.
[8] G. P. Agrawal, *Fiber-Optic Communication Systems*. New York: Wiley, 1997.
[9] A. S. Daryoush, K. Sato, K. Horikawa, and H. Ogawa, "Dynamic response of long optical-cavity laser diode for Ka-band communication satellites," *IEEE Trans. Microwave Theory Tech.*, vol. 45, pp. 1288–1295, 1997.
[10] S. Fukushima, Y. Doi, T. Ohno, Y. Matsuoka, and H. Takeuchi, "New phase-shift keying technique based on optical delay switching for microwave optical link," *IEEE Photon. Technol. Lett.*, vol. 11, pp. 1036–1038, 1999.
[11] D. Wake, C. R. Lima, and P. A. Davies, "Transmission of 60-GHz signals over 100 km of optical fiber using a dual-mode semiconductor laser source," *IEEE Photon. Technol. Lett.*, vol. 8, pp. 578–580, 1996.

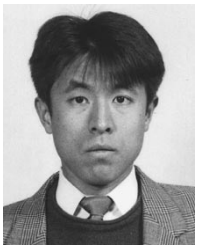

Tetsuichiro Ohno (M'98) was born in Osaka, Japan, in 1966. He received the B.E. and M.E. degrees from Osaka University in 1989 and 1991, respectively, and the Ph.D. degree from Shizuoka University, Japan, in 1999.

In 1991, he joined NTT Opto-electronics Laboratories, Kanagawa, Japan, where he has been engaged in opto-electronic devices. His current interests are in the area of optical devices used in fiber-radio systems.

Dr. Ohno is a member of the IEEE Lasers and Electro-Optics Society (LEOS).

Kenji Sato (M'95) received the B.S., M.S., and Ph.D. degrees from Nagoya University, Nagoya, Japan, in 1978, 1980, and 1992, respectively.

In 1980, he joined NTT Electrical Communications Laboratories, Japan. He is now a Senior Research Engineer with NTT Network Innovation Laboratories, Kanagawa, Japan. His current interests include optical short-pulse sources and its applications to high-speed fiber transmission systems.

Dr. Sato is a member of the IEEE Lasers and Electro-Optics Society (LEOS), the Physical Society of Japan, the Japan Society of Applied Physics, and the Institute of Electronics, Information, and Communications Engineers (IEICE) of Japan.

Seiji Fukushima was born in Kumamoto, Japan, in 1962. He received the B.S., M.S., and Ph.D. degrees in electrical engineering from Kyushu University, Japan, in 1984, 1986, and 1993, respectively.

In 1986, he joined the NTT Opto-electronics Laboratories, Japan, where he was engaged in research of spatial light modulators and optical computing systems. From 1995 to 1997, he was engaged in research of high-speed optical interconnection for the integrated circuits in the NTT System Electronics Laboratories, Japan. In 1997, he began studying devices for the fiber-radio access systems in NTT Photonics Laboratories.

Dr. Fukushima is a member of the Optical Society of America (OSA), the Institute of Electronics, Information, and Communications Engineers (IEICE) of Japan, and the Japan Society of Applied Physics.

Yoshiyuki Doi received the B.S. and M.S. degrees from Shinshu University, Nagano, Japan, in 1995 and 1997, respectively.

In 1997, he joined NTT Opto-electronics Laboratories, Kanagawa, Japan, where he has been engaged in optical devices used in fiber-radio systems.

Mr. Doi is a member of the Institute of Electronics, Information, and Communications Engineers (IEICE) of Japan.

Yutaka Matsuoka (M'92) received the B.S. and M.S. degrees in physics from Tokyo Institute of Technology, Tokyo, Japan, in 1974 and 1976, respectively.

In 1976, he joined the NTT Musashino Electrical Communication Laboratory, Japan, where he worked on electrical characterization of Si and GaAs substrates. From 1982 to 1986, his research focused on high-speed GaAs MESFET's and IC's. He is currently with NTT Photonics Laboratories, Kanagawa, Japan, where his research interests include high-performance photodiodes, InP-based heterostructure bipolar transistors, OEIC's, and microwave/millimeter (mm)-wave photonics.